Photolysis of Segmented Polyurethanes. The Role of Hard-Segment Content and Hydrogen Bonding

CHARLES E. HOYLE, KYU-JUN KIM, Y. G. NO, and G. L. NELSON, *Department of Polymer Science, University of Southern Mississippi, Southern Station 10076, Hattiesburg, Mississippi 39406-0076*

Synopsis

The photodegradation of segmented polyurethanes based on methylene 4,4'-diphenyldiiso-cyanate (MDI) is shown to be dependent on the physical structure of the polymer. As the hard segment content of the polyurethane is increased, the photodegradation efficiency is lowered. In particular, the extent of the photolytic decomposition is inversely dependent on the degree of hydrogen bonding in the aryl carbamate groups in the polyurethane backbone. Utilizing appropriate model compounds for comparison, the formation of the ortho photo-Fries rearrangement product, as detected by fluorescence spectroscopy, is also shown to be dependent on the degree of hydrogen bonding. In general, the restrictive mobility imposed by hydrogen bonding is a critical factor which must be considered in the photochemistry of segmented polyurethanes.

INTRODUCTION

Since their first introduction, polyurethanes based on aromatic diisocyantes have been employed in a wide variety of commercial applications. However, when used in coatings applications aromatic diisocyanate-based polyurethanes (hereafter called aromatic polyurethanes) show low resistance to ultraviolet radiation.[1] As a result, in many cases aromatic polyurethanes have been relegated to limited use in favor of the more expensive aliphatic diisocyanate-based polyurethanes.

Two primary schemes (shown below) have been proposed to account for the photodegradation of aromatic polyurethanes. One[2-7] results in the formation of colored quinoid products (Scheme I) while the other (Scheme II) yields
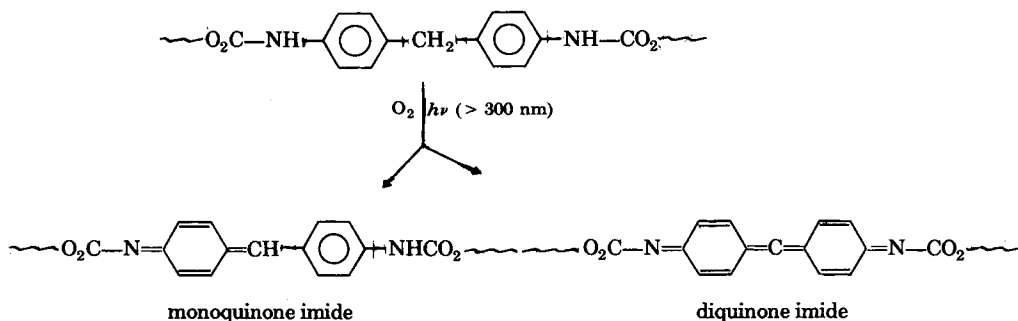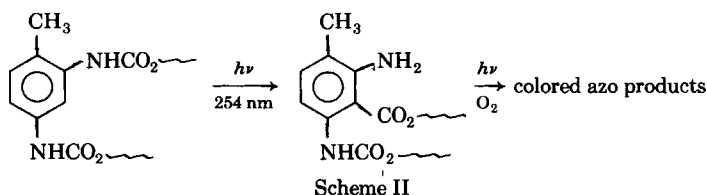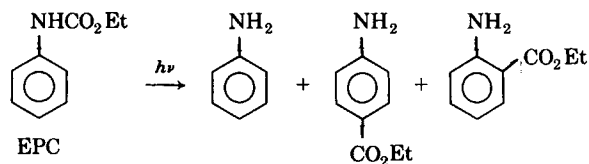

Scheme I

photo-Fries rearrangement and cleavage-type products.[8] Once formed, the photo-Fries products could then yield, upon photolysis, colored azo compounds (Scheme II).

Scheme II

Both schemes account for the ultimate discoloration of aromatic polyurethanes. In support of the photo-Fries mechanism, several research groups using model compounds such as ethyl N-phenyl carbamate (EPC) (see Scheme III below) have found that indeed photolysis of aryl carbamates gives photo-Fries products:[8-15]

Scheme III

In a recent account, Gardette and Lemaire[17-19] suggest that either the quinoid type structures or the photo-Fries products may form depending on the wavelength of excitation as shown in Scheme IV:

Scheme IV
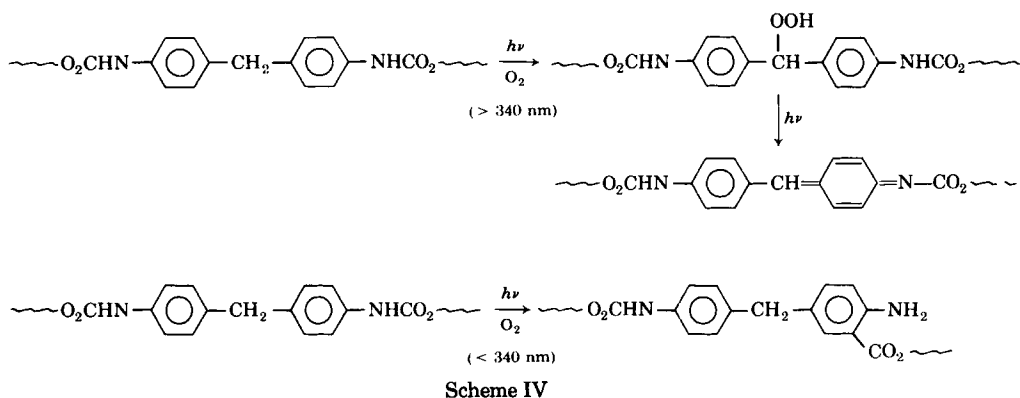
Despite the number of reports on the photolysis of aromatic polyurethanes and related model compounds, few if any deal with the effect of the polyurethane structure and physical state on the photodegradation process. In this paper, we present results for the photolysis of aromatic polyurethane segmented elastomers showing that the photolysis process is directly related to the "hard–soft" segment content of the polyurethane. In particular, it is demonstrated that the photodegradation can readily be related to the extent

of hydrogen bonding in the segmented polymer. First, results for the steady-state and time-resolved fluorescence analysis of small molecule aryl carbamates are presented to establish the role of the photo-Fries rearrangement process in the photolysis of model aryl carbamates in solution. Then the fluorescence analysis procedure is extended to studies of model biscarbamates and segmented aromatic polyurethanes.

EXPERIMENTAL

Methylene 4,4′-diphenyldiisocyanate (MDI-Mobay) was recrystallized before use. 1,4-Butanediol (Aldrich) used in polyurethane preparation was distilled prior to use. Poly(ethylene oxide) (PEO) (Aldrich) and poly(tetramethylene oxide) (PTMO) (Polyscience) were dehydrated under a rough vacuum at 50°C for 1 day. Polyurethane elastomers were prepared by a prepolymer method.[20]

The segmented polyurethane elastomer films were cast on aluminum dishes from DMF. For percent gel formation and absorbance changes of films, as well as the fluorescence lifetime measurements of photolyzed solutions, photolysis was performed with either 300 or 350 nm lamps (Rayonet reactor) for various time periods. For the percent gel formation determinations, the photolyzed films were dissolved in hot DMF and the insoluble gel was collected, dried in a vacuum oven, and weighed. The films subjected to fluorescence analysis were photolyzed with a xenon lamp (150 W)/monochromator combination at 280 nm with 5 nm monochromator slit widths.

Steady state fluorescence spectra were recorded using a Perkin-Elmer fluorescence spectrometer Model 650-10S. The fluorescence decay curves were obtained with a single-photon-counting apparatus from Photochemical Research Associates (PRA). The data were analyzed by a software package from PRA based on the iterative convolution method. UV spectra were recorded on a Perkin-Elmer 320 dual-beam spectrophotometer. The thermal transitions of the polymers were examined with a DuPont 910 differential scanning calorimeter. ET-IR spectra were recorded on a Nicolet Instrument Corporation 1200 S.

RESULTS AND DISCUSSION

The results and discussion section is divided into two parts. The first deals with photolysis of model aryl carbamates and biscarbamates and establishes the background and methods to aid in interpretation of the results for the segmented polyurethanes. The second part presents results for the photolysis of segmented aromatic polyurethanes and relates the hard segment content and degree of hydrogen bonding in the polyurethane to the extent and mechanism of degradation.

Photolysis of Model Aryl Mono- and Biscarbamates. Judging from the reported products produced by the well-studied photolysis of EPC (depicted in Scheme III), one would expect a photolyzed solution of EPC to give a well-defined and quite characteristic fluorescence emission spectrum. In an earlier report, we have shown that the steady-state fluorescence of EPC is totally lost upon photolysis (300 nm lamps of a Rayonet reactor) and replaced by two new emission peaks, one with a maximum at ~ 340 nm and the other with a maximum above 400 nm.[21] The fluorescing species have been tenta-
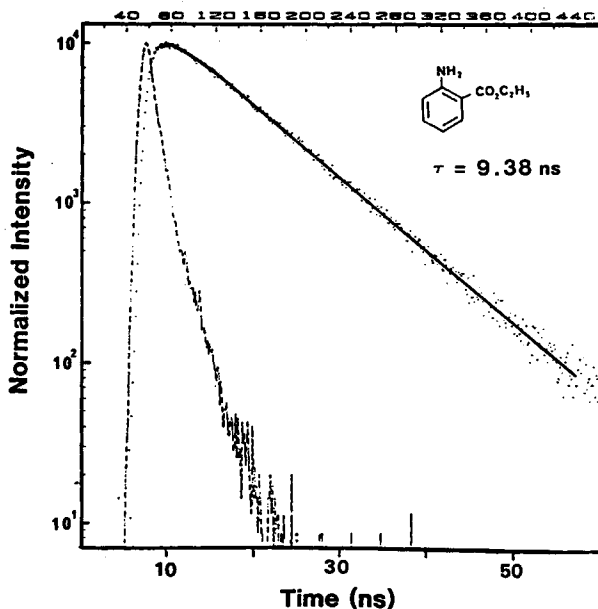
Fig. 1. Fluorescence decay curve (N_2) of $2 \times 10^{-4}M$ solution of ethyl 2-amino benzoate in DMF: λ_{ex} = 330 nm; λ_{em} = 420 nm.

tively assigned (see Ref. 21) by comparison with the steady-state fluorescence of authentic samples of the photo-Fries products of EPC. Figure 1 gives the fluorescence decay curve (λ_{em} = 420 nm, N_2) of ethyl 2-aminobenzoate (hereafter referred to as the ortho photo-Fries product of EPC) with a single exponential decay time of 9.38 ns in DMF. Comparing the fluorescence decay time of 9.34 ns (Fig. 2) obtained by monitoring the photolyzed EPC solution in
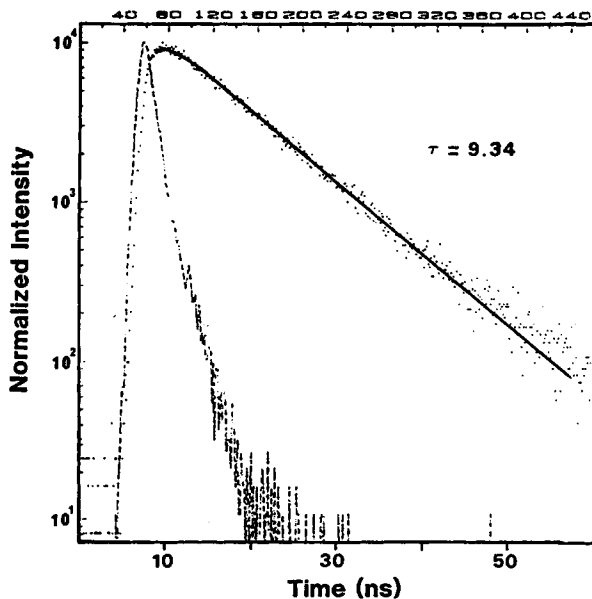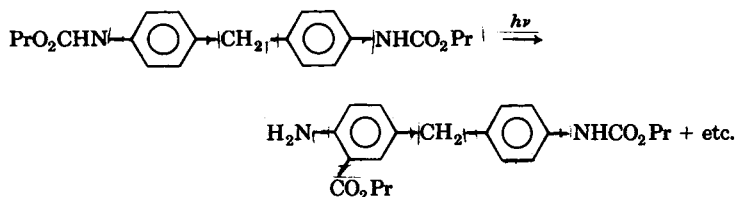

Fig. 2. Fluorescence decay curve (N_2) of photolyzed (Rayonet reactor, 300 nm lamps, 1 h, air) $2.4 \times 10^{-4}M$ solution of ethyl N-phenyl carbamate in DMF: λ_{ex} = 330 nm; λ_{em} = 420 nm.

air at 420 nm gives positive identification of the ortho photo-Fries as the species responsible for the red-shifted emission with maximum above 400 nm.

In addition to the EPC model, we have also analyzed the photolysis of a model biscarbamate of MDI (shown below):

$$PrO_2CHN\!\!-\!\!\langle\bigcirc\rangle\!\!-\!\!|CH_2|\!\!-\!\!\langle\bigcirc\rangle\!\!-\!\!|NHCO_2Pr \ | \overset{h\nu}{\Longrightarrow}$$

$$H_2N\!\!-\!\!\langle\bigcirc\rangle\!\!-\!\!|CH_2|\!\!-\!\!\langle\bigcirc\rangle\!\!-\!\!NHCO_2Pr + etc.$$
$$\underset{CO_2Pr}{}$$

Like EPC, the photolysis of the model biscarbamate (1 h, Rayonet reactor, 300 nm lamps, air) gives a steady-state emission spectrum with red-shifted maximum above 410 nm with the long-lived component of the fluorescence decay curve (fit to a double exponential decay function) having a lifetime of 9.97 ns. Comparison with the 11.1 ns (1.5×10^{-4} DMF) decay time of propyl 2-amino 5-methylbenzoate (PAMB), a model ortho photo-Fries product which is para-methyl-substituted, leads to the conclusion that photolysis of the model biscarbamate of MDI also results in ortho photo-Fries product forma-

TABLE I
Photophysical Data for Photolyzed Model Aryl Carbamates

Compound	Photolysis conditions	λ_{max} (nm)[e]	Lifetime (ns)
NH$_2$ / CO$_2$C$_2$H$_5$ [a]	Unphotolyzed	405	9.38[f]
NH$_2$ / CO$_2$Pr [b] / CH$_3$	Unphotolyzed	416	11.1[f]
NHCO$_2$C$_2$H$_5$ [c]	Photolyzed—1 h in Rayonet reactor (300 nm lamps)	402	9.34[f]
CH$_2$+(⬡)—$\overset{H}{N}$CO$_2$Pr$)_2$ [d]	Photolyzed—1 h in Rayonet reactor (300 nm lamps)	402	9.97[g]

[a] $2 \times 10^{-4}M$ in DMF.
[b] $1.7 \times 10^{-4}M$ in DMF.
[c] Unphotolyzed sample is $2.4 \times 10^{-4}M$ in DMF.
[d] Unphotolyzed sample is $9 \times 10^{-5}M$ in DMF.
[e] Emission maximum recorded; uncorrected for instrumental spectral response.
[f] Decay curve fit to single exponential decay function.
[g] Long-lived component of decay curve.

tion when photolyzed in solution. The results for photolysis of EPC and the MDI biscarbamate model are compiled in Table I along with the appropriate entries for the two authentic photo-Fries compounds utilized for comparison. Similar data to those reported in this paper for EPC photolysis have been found for other mono- and bisarylcarbamates which suggests that the ortho photo-Fries product formation is a general reaction for photolysis of arylcarbamates.[12,16] The results derived from this section on model compound studies will be utilized, along with UV spectral and gel percent measurements, to analyze the photolysis of actual segmented aromatic diisocyanate based on polyurethane films.

Photolysis of Segmented Polyurethanes Based on MDI—Chain Flexibility Effects Using UV, Gel, and Fluorescence Analysis. In this section, results are presented for the effect of chain flexibility and hydrogen bonding on the photolysis of a series of segmented polyurethanes based on MDI and various polyether polyols which are chain extended with 1, 4-butanediol (BDO). Two sets of polyurethanes were synthesized for this study by the standard prepolymer method.[20] The first set is a series of MDI/1,4-butanediol (BDO)/poly(tetramethylene oxide) (PTMO—average molecular weight 1000) polymers with varying hard segment (1, 4-butanediol extender) content. In the first series of polymers, names are based on the ratio of MDI : BDO : PTMO. For example, a polymer comprised of 4 parts MDI, 3 parts BDO, and 1 part PTMO would be named PU–PTMO 4 : 3 : 1 indicating that it is an elastomeric polyurethane (PU) based on poly(tetramethylene oxide) (PTMO) with molecular weight 1000 and an MDI : BDO : PTMO ratio of 4 : 3 : 1. The second series are based on MDI and poly(ethylene oxide) (PEO) with the 1, 4-butanediol extender. In this series, the ratio of MDI : BDO : PEO is 2 : 1 : 1 for each polymer, and names are based on the PEO molecular weight. Thus, the segmented polyurethane comprised of 2 parts MDI, 1 part 1, 4-butanediol, and 1 part PEO (average molecular weight of 300) is PU–PEO 300. The other polymer in this series is named accordingly PU–PEO 600. A generalized structure of the segmented polyurethanes utilized in this section is shown below.
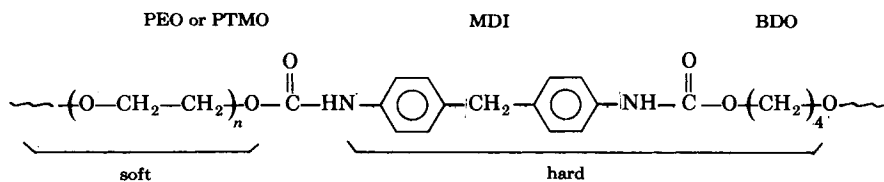
The soft segment may either have ethylene oxide (as shown) or tetramethylene oxide repeat units. In keeping with the traditional view of segmented polyurethanes, the soft and hard segments are identified as the polyol and the MDI/BDO region, respectively. Results are presented first for the PTMO based polyurethanes.

Figure 3 shows results for the change in the absorbance at 400 nm (selected to illustrate the absorbance buildup in the far UV/near visible region) upon photolysis of two MDI–PTMO-based polyurethane films. The polyurethane represented by curve *a* has a ratio of MDI : BDO : PTMO of 2 : 1 : 1
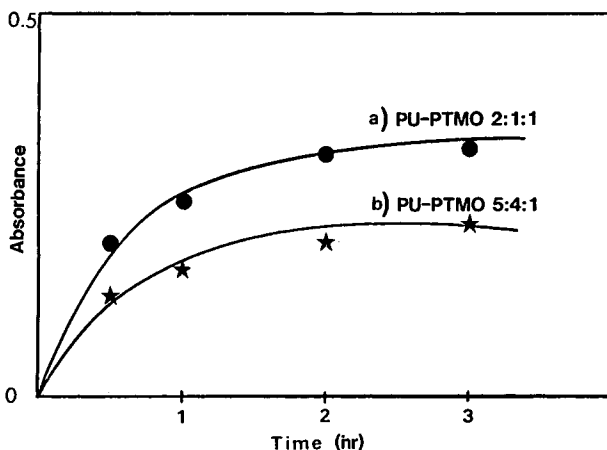
Fig. 3. UV absorbance changes (recorded at 400 nm) as a function of photolysis time (Rayonet reactor, 300 nm lamps) for (a) PU–PTMO 2:1:1 and (b) PU–PTMO 5:4:1 films in air.

(PU–PTMO 2:1:1) while curve *b* is for a polyurethane with MDI:BDO:PTMO of 5:4:1 (designated PU–PTMO 5:4:1). Even though the PU–PTMO 5:4:1 polymer has a significantly higher concentration of carbamate chromophores, its rate of absorbance increase with photolysis time is less than for the PU–PTMO 2:1:1 polyurethane. Apparently the larger content of hard segments in the PU–PTMO 5:4:1 polymer retards the photodegradation process. Similar results have been found for increase in gel content, i.e., photolysis of PU–PTMO 5:4:1 for a given time results in a lower production of insoluble gel than for PU–PTMO 2:1:1. In fact, Figure 4 shows that in general as the hard segment concentration increases (increasing BDO content) the extent of insoluble gel formed upon photolysis (8 h, Rayonet reactor, 300 nm lamps, air) decreases. Interestingly, there is a large drop (by almost half) in the gel percent going from the PU–PTMO 2:1:1 polymer to the PU–PTMO 3:2:1 polymer followed by a leveling off with
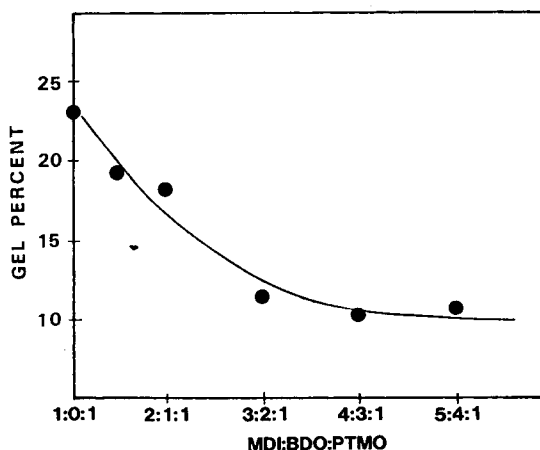

Fig. 4. Gel percent formation vs. hard-segment content on photolysis (Rayonet reactor, 300 nm lamps, 8 h, air) of PU–PTMO polyurethane films in air.
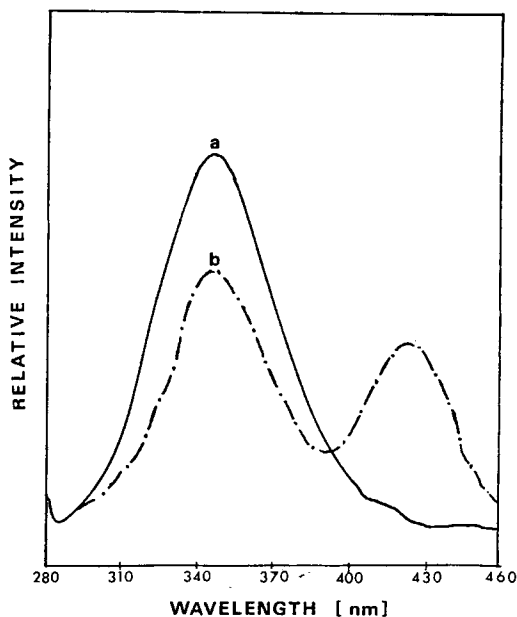
Fig. 5. Fluorescence spectral change ($\lambda_{ex} = 280$ nm) on photolysis (Rayonet reactor, 300 nm lamps, 30 min, air) of PU–PEO 300 (0.01 g/dL) and/or PU–PEO 600 (0.005 g/dL) in DMF solution: (a) 0 min photolysis; (b) 30 min photolysis.
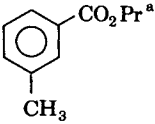
increasing BDO content. The decrease in photolytic reactivity of the segmented polyurethanes correlates with the increase in hard segment (MDI–BDO portion) content of the polymer. This is due to a decrease in polymer flexibility and/or an increase in hydrogen-bonded carbonyl with increasing hard segment concentration in the polyurethane backbone. (This concept will be explored further in the next few paragraphs in an investigation of the photolysis of the PEO-based polyurethanes).

Before discussing the results for photolysis of the PU–PEO films in the solid state, it should be noted that the photolysis of PU–PEO 300 and PU–PEO 600 in DMF solution (30 min, 300 nm lamps, Rayonet reactor, air) gives a new fluorescence emission (curve b, Fig. 5) above 400 nm. The long-lived lifetime components of the emission above 400 nm are approximately 10.7 and 10.0 ns for the photolyzed PU–PEO 300 and PU–PEO 600 solutions (Table II). By comparison with the lifetime of the model photo-Fries product (propyl 2-amino 5-methylbenzoate) shown in Table II, the emission above 400 nm can be assigned (at least in part) to an ortho photo-Fries type product. These results are also consistent with the lifetime for the photolyzed biscarbamate solution in Table I and provide further evidence for formation of the ortho photo-Fries product in the PU–PEO 300 and PU–PEO 600 solutions.

Photolysis of the PU–PEO 300 and PU–PEO 600 films in air, as opposed to the solution photolysis, gave quite different results. The photolyzed PU–PEO 300 film (Fig. 6) showed no, or at least very little, new emission above 400 nm. By contrast, the photolyzed PU–PEO 600 film (Fig. 7) is characterized by a new emission above 400 nm which has a multiexponential decay curve.

TABLE II
Photophysical Data for Photolyzed PU–PEO 300 and PU–PEO 600 Solutions

Compound	Photolysis conditions	λ_{max} (nm)[d]	Lifetime (ns)
NH$_2$ ⎯⎯ CO$_2$Pr [a] ⎯⎯ CH$_3$	Unphotolyzed	416	11.1[e]
PU–PEO 300[b]	Photolyzed—30 min in Rayonet reactor (300 nm lamps, N$_2$)	425	10.7[f]
PU–PEO 600[c]	Photolyzed—30 min in Rayonet reactor (300 nm lamps, N$_2$)	425	10.0[f]

[a]$1.7 \times 10^{-4}M$ in DMF.
[b]Unphotolyzed sample is 0.01 g/dL in DMF.
[c]Unphotolyzed sample is 0.005 g/dL in DMF.
[d]Emission maximum recorded; uncorrected for instrumental spectral response.
[e]Decay curve fit to single exponential decay function.
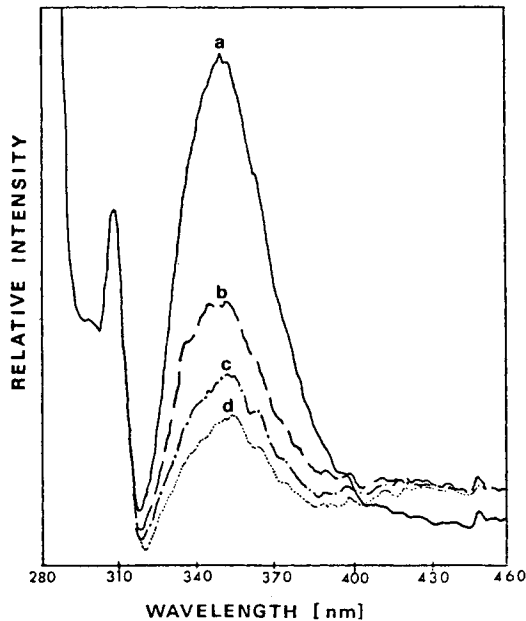[f]Long-lived component of decay curve.

Fig. 6. Fluorescence spectral change (λ_{ex} = 285 nm) on photolysis (285 nm, Xenon lamp/monochromator) of PU–PEO 300 film in air: (a) 0 min photolysis; (b) 20 min photolysis; (c) 40 min photolysis; (d) 60 min photolysis.
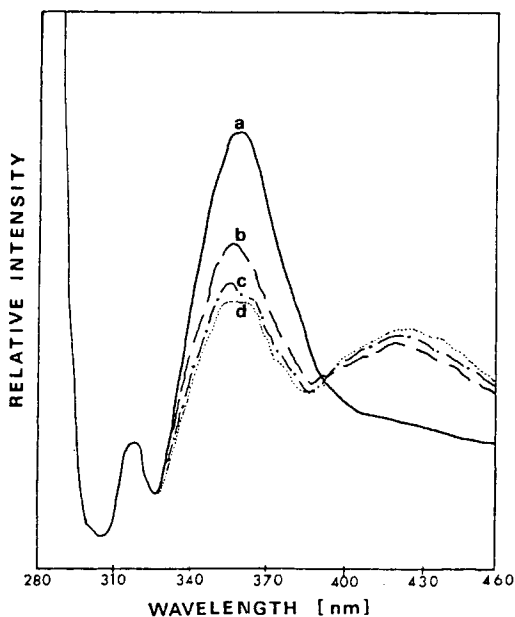
Fig. 7. Fluorescence spectral change (λ_{ex} = 285 nm) on photolysis (285 nm, Xenon lamp/monochromator) of PU–PEO 600 film in air: (a) 0 min photolysis; (b) 20 min photolysis; (c) 40 min photolysis; (d) 60 min photolysis.

Although positive identification of all of the species contributing to the emission above 400 nm in Figure 7 cannot be made, the important fact is that the photolyzed PU–PEO 600 shows the new emission above 400 nm while PU–PEO 300 does not.

Results are shown in Figure 8 for the increase in gel formation upon photolysis (Rayonet reactor, 300 nm lamps) of PU–PEO 300 and PU–PEO 600 films in air. As the molecular weight of the PEO soft segment doubles, the percent insoluble gel formed increases. How can these results be explained?
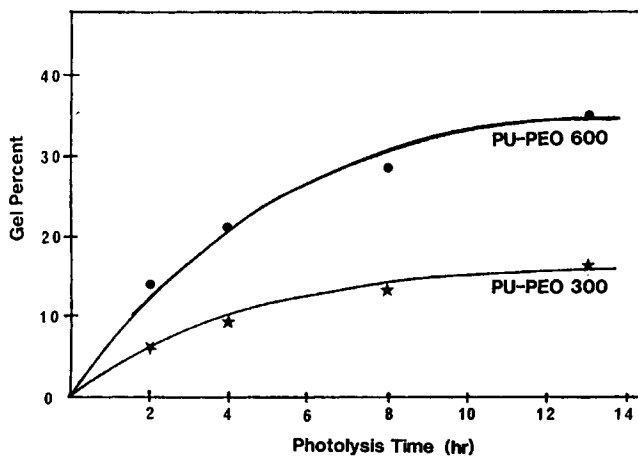

Fig. 8. Gel percent formation vs. photolysis time (Rayonet Reactor, 300 nm lamps) for PU–PEO 300 and PU–PEO 600 films in air.
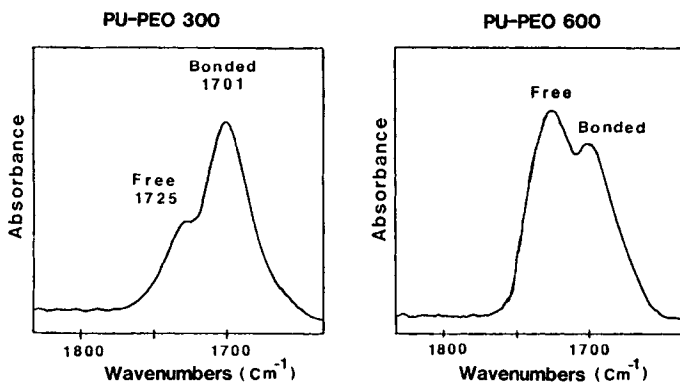
Fig. 9. IR spectra of PU–PEO 300 and PU–PEO 600 films.

One might first turn to a crystallinity argument. However, DSC and X-ray diffraction analysis of the segmented polymers show little or no crystallinity for either PU–PEO 300 or PU–PEO 600. Consideration of the increasing flexibility of the soft segment on going from PU–PEO 300 to PU–PEO 600 no doubt accounts for some difference in behavior. And certainly oxygen, which is necessary (as demonstrated in another paper in this series[22]) to the crosslinking process, might be expected to diffuse faster in the PU–PEO 600 than in the PU–PEO 300 film. But a most compelling argument involves the dramatic difference in the nature of the hydrogen-bonding characteristics of the two segmented polyurethanes under consideration. The FT-IR spectra of PU–PEO 300 and PU–PEO 600 (Fig. 9) reveal a hydrogen-bonded carbonyl (1705 cm^{-1}) and a nonbonded or free carbonyl (1725 cm^{-1}) (see Ref. 23 for discussion of this phenomena). In the case of PU–PEO 300, there is a significant degree of hydrogen bonding to the carbonyl in the urethane moiety. PU–PEO 600, on the other hand, has primarily nonbonded carbonyl and is free to move. This could well account for the lower yield of gel content on photolysis of PU–PEO 300. The carbonyl radical formed by an N—C bond cleavage in the excited urethane group, if restricted by hydrogen bonding, might be less likely to lead to photodegradation. The hydrogen-bonding argument in general calls for restrictive local mobility and such would be expected to inhibit processes leading to crosslinking (gel formation).

In summary, it is not difficult to imagine that the reduced degradation of PU–PEO 300 results from a decrease in flexibility due both to hydrogen bonding as well as the inherent shorter length of the PEO soft segment. Of course, both factors are closely related and difficult to differentiate between. Finally, the argument advanced for the differences in the PU–PEO films can be extended to the PU–PTMO polymers. The decrease in gel formation upon photolysis of the PU–PTMO polyurethanes with higher hard segment content is probably due to an increase in hydrogen bonding and decrease in chain flexibility.

CONCLUSIONS

Results for the photolysis of segmented polyurethanes [based on MDI, an aliphatic diol (1,4-butanediol) and appropriate polyols] have been presented

with emphasis on the effect of physical structure of the film on the photo-degradation process. The following general conclusions can be drawn from the results in this paper:

1. The photodegradation of segmented aromatic polyurethanes is directly related to the hard segment content of the polymers.

2. The photolytic degradation of segmented aromatic polyurethanes is inversely related to the extent of hydrogen bonding in the carbamate chromophores.

3. The photolysis of model aryl carbamates can be effectively utilized in the study of aromatic polyurethanes.

References

1. Z. Osawa, *Developments in Polymer Photochemistry*, N. S. Allen, Ed., Applied Science, London, 1982, Vol. 3, p. 209.

2. C. S. Schollenberger and K. Dinsbergs, *Soc. Plast. Eng. Trans*, 1, 31 (1961).

3. C. S. Schollenberger, L. G. Pappas, J. C. Park, and V. V. Vickroy, *Rubber World*, 139, 81 (1960).

4. L. V. Nevskii, O. Tarakanov, and V. Belyakov, *Sov. Plast.*, 9, 47 (1967).

5. L. Nevskii, O. Tarakanov, and V. Belyakov, *Sov. Plast.*, 10, 23 (1967).

6. L. Nevskii, O. Tarakanov and V. Belyakov, *J. Polym. Sci. Part C*, 23, 1193 (1968).

7. O. G. Tarakanov, L. B. Nevskii, and A. P. Kafengauz, *Sov. Plast.*, 1, 46 (1972).

8. H. C. Beachell and L. C. Chang, *J. Polym. Sci.*, A-1, 10, 503 (1972).

9. D. Bellus and K. Schaeffer, *Helv. Chim. Acta.*, 51, 221 (1968).

10. K. Schwetlick, J. Stumpe, and R. Noack, *Tetrahedron*, 35, 63 (1979).

11. K. Schwetlick, R. Noack, and G. Schmieder, *Z. Chem.*, 12, 107 (1972).

12. C. E. Hoyle, T. B. Garrett, and J. E. Herweh, *Photodegradation and Photostabilization of Coatings*, S. P. Pappas and F. H. Winslow, Eds., ACS Symposium Series 151, 1981.

13. C. E. Hoyle and J. E. Herweh, *J. Org. Chem.*, 11, 2195 (1980).

14. D. Masilamani, R. O. Hutchins, and J. Ohr, *J. Org. Chem.*, 41, 3687 (1976).

15. D. J. Trecker, R. S. Foote, and C. L. Osborn, *Chem. Commun.*, 1034 (1968).

16. H. Schulze, *Z. Naturforsch.*, B28, 339 (1973).

17. J. L. Gardette and J. Lemaire, *Makromol. Chem.*, 182, 2723 (1981).

18. J. L. Gardette and J. Lemaire, *Makromol. Chem.*, 183, 2415 (1982).

19. J. L. Gardette and J. Lemaire, *Polym. Deg. Stab.*, 6, 135 (1984).

20. J. H. Saunders and K. C. Frisch, *Polyurethanes: Chemistry and Technology*, Wiley-Interscience, New York, 1962, Vol. XVI, p. 273.

21. C. E. Hoyle and K. J. Kim, *J. Polym. Sci. Polym. Chem. Ed.*, 24, 1879 (1986).

22. C. E. Hoyle and Y. G. No, to appear.

23. R. W. Seymour, G. M. Esters, and S. L. Cooper, *Macromolecules*, 3(5), 579 (1970).